

Magnetic Nanosized $\{M^{II}_{24}\}$ -Wheel-Based ($M = Co, Ni$) Coordination Polymers

Jia Li, Jun Tao,* Rong-Bin Huang, and Lan-Sun Zheng

State Key Laboratory of Physical Chemistry of Solid Surfaces and Department of Chemistry, College of Chemistry and Chemical Engineering, Xiamen University, Xiamen 361005, People's Republic of China

S Supporting Information

ABSTRACT: Two 3D coordination polymers, $[Co_{24}(OH)_{12}(SO_4)_{12}(ip)_6(DMSO)_{18}(H_2O)_6] \cdot (DMSO)_6 \cdot (EtOH)_6(H_2O)_{36}$ (**1**-guests, ip = isophthalate) and $[Ni_{24}(OH)_{12}(SO_4)_{12}(ip)_6(DMSO)_{12}(H_2O)_{12}] \cdot (DMSO)_6 \cdot (EtOH)_6(H_2O)_{20}$ (**2**-guests), constructed with nanosized tetraicosanuclear Co^{II} and Ni^{II} wheels are solvothermally synthesized. Both complexes show intra- and interwheel dominant antiferromagnetic interactions.

High-nuclearity clusters have attracted much attention because of their intriguing structures and fascinating chemical and physical properties. If possessing large-spin ground states and easy-axis magnetic anisotropy, they can behave as single-molecule magnets that link the microscopic and macroscopic worlds as well as quantum and classical systems.¹ On the other hand, when acting as structural and/or functional building units and being assembled into 1D–3D networks, they can endow such networks with expected topological structures and physical properties.² Among the high-nuclearity clusters, molecular magnetic wheels are of particular importance not only because they usually possess inherent structural beauty but also because they represent ideal model systems for the studies of 1D magnetism, spin frustration, magnetic anisotropy, and quantum effects.³ Up to now, several homometallic discrete compounds composed of Ni_{24} ,⁴ Fe_{18} ,⁵ Co_{24} ,⁶ Cu_{16} ,⁷ Mn_{84} ,⁸ and Mo_{176} ⁹ wheels have been reported. The formation of these wheels, although seemingly serendipitous, reveals a prevalent feature that the metal ions are bridged by oxo, hydroxyl, and/or alkoxy groups produced via hydrolysis and alcoholysis reactions of metal salts in the presence of supporting organic ligands (except Mo_{176}), which hints that such wheels can be assembled into coordination polymers if the supporting organic ligands are polytopic. However, coordination polymers with molecular wheel building units are unexpectedly rare. To our knowledge, only two wheel-based coordination polymers, $Ti_8O_8(OH)_4(tp)_6$ (tp = terephthalate) and $Be_{12}(OH)_{12}(BTB)_6$ (BTB = 1,3,5-benzenetribenzoate), were recently reported.¹⁰ As part of our interest in high-nuclearity clusters of paramagnetic ions and metal-cluster-based coordination polymers, we report herein two new complexes, $[Co_{24}(OH)_{12}(SO_4)_{12}(ip)_6(DMSO)_{18}(H_2O)_6] \cdot (DMSO)_6 \cdot (EtOH)_6(H_2O)_{36}$ (**1**-guests) and $[Ni_{24}(OH)_{12}(SO_4)_{12}(ip)_6(DMSO)_{12}(H_2O)_{12}] \cdot (DMSO)_6 \cdot (EtOH)_6(H_2O)_{20}$ (**2**-guests); both are 3D coordination polymers constructed with nanosized tetraicosanuclear metal-ion wheel units.

The formation of the two wheel units apparently involves the hydrolysis of Co^{II} and Ni^{II} ions under solvothermal conditions (Supporting Information) assisted by sulfate ions, ip ligands, and even solvent molecules. It is possible that sulfate ion hereinto plays a more important role in the hydrolysis of Co^{II} and Ni^{II} ions and in the formation of wheel structural units because its relatively strong coordination ability compared with perchlorate, nitrate, or hydrogen phosphate ion, whose Co^{II} and Ni^{II} salts, however, could not give wheel structures under the same reaction conditions.

Both complexes crystallize in the trigonal space group $R\bar{3}$ and are composed of nanosized M^{II}_{24} wheels with diameter of ~ 2.0 nm (Figure 1a). The solvent molecules could not be located in the structures; their amounts are determined by elemental analysis. The M^{II}_{24} wheel lies on a crystallographic 3-fold axis and an inversion center, with the asymmetric unit containing four distinct M^{II} ions, one ip^{2-} ligand, and two μ_3-OH^- and two $\eta^1:\eta^1:\eta^2:\mu_3-SO_4^{2-}$ groups (Figure 1b,c). Besides, three DMSO molecules, of which two serve as μ bridges, and one water molecule are also coordinated to Co^{II} ions in **1**, while in **2**, the molecule that is η^1 -DMSO in **1** is here replaced with a water molecule (O2W on Ni4 atom). The four M^{II} ions in the asymmetric unit can be viewed as a defected cubane, $M_3(\mu_3-O_5)$, connected to the fourth one. All M^{II} ions lie in distorted octahedra formed with six O atoms. In **1**, the O atoms around the Co1 ion derive from two ip carboxylate groups (O1 and O4A), one μ_3-OH^- group (O6D), and one η^1 -DMSO (O15) and two $\mu-O$ from two SO_4^{2-} groups (O7 and O11); the Co2 ion is coordinated by one O atom (O2) from an ip carboxylate group, one μ_3-OH^- group (O5), two $\mu-O$ atoms (O16 and O17) from two DMSO molecules, and two $\mu-O$ atoms (O7 and O11) from two SO_4^{2-} groups. The Co3 ion does not coordinate to the ip ligand, whose coordination sphere is formed by O atoms from two μ_3-OH^- groups (O5 and O6), two SO_4^{2-} groups (O10C and O12C), one μ -DMSO (O16), and one water molecule (O1W), while the Co4 ion is coordinated by one ip carboxylate group (O3B), two μ_3-OH^- groups (O5 and O6), one μ -DMSO (O17), and two SO_4^{2-} groups (O8C and O13). The average bond lengths for Co1, Co2, Co3, and Co4 are 2.089, 2.103, 2.095, and 2.112 Å, respectively. In **2**, the average Ni–O bond distances are 2.067, 2.052, 2.064, and 2.056 Å for Ni1, Ni2, Ni3, and Ni4, respectively. The anions or ligands in the wheels coordinate in diverse modes, showing M–O bond lengths in a sequence of

Received: March 4, 2012

Published: May 24, 2012



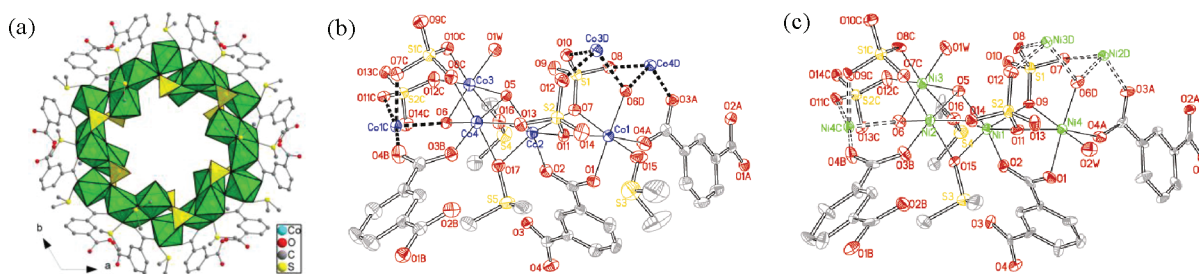


Figure 1. Perspective view of the M^{II}_{24} wheel showing edge- and vertex-sharing $M^{II}O_6$ (green) and SO_4 (yellow) polyhedra (a) and the asymmetric structural units in coordination polymers **1** (b) and **2** (c), respectively. Symmetry codes: A, $x - y + 2/3, x - 2/3, -z + 7/3$; B, $-y + 4/3, x - y - 1/3, z - 1/3$; C, $x - y, x - 1, -z + 2$; D, $y + 1, -x + y + 1, -z + 2$ for **1**; A, $x - y + 1/3, x + 2/3, -z + 2/3$; B, $-y + 1/3, x - y + 2/3, z - 1/3$; C, $x - y + 2/3, x + 1/3, -z + 1/3$; D, $y - 1/3, -x + y + 1/3, -z + 1/3$ for **2**.

$d(\mu-O, DMSO) > d(\mu-O, SO_4^{2-}) > d(\eta^1-O, DMSO) > d(\eta^1-O, SO_4^{2-}) > d(\mu_3-OH^-) > d(\eta^1:\eta^1:\mu-O, COO^-)$ for **1** and $d(\mu-O, SO_4^{2-}) > d(\mu-O, DMSO) > d(\eta^1-O, DMSO) > d(\eta^1-O, SO_4^{2-}) > d(\mu_3-OH^-) > d(\eta^1:\eta^1:\mu-O, COO^-)$ for **2**, respectively (Table S2 in the Supporting Information).

The asymmetric M^{II}_4 units are linked to their symmetry-related ones (dotted lines in Figure 1b,c) by μ_3-OH^- ions, $\eta^1:\eta^1:\eta^2:\mu_3-SO_4^{2-}$ groups, and ip carboxylate groups, respectively, resulting in an overall M^{II}_{24} wheel that consists of six edge- and vertex-sharing $\{M^{II}O_6\}_4$ species (Figure 1a). The M^{II}_{24} wheel can be viewed as nanosized building units (Figure 2a) above and below which they are capped with peripheral ip

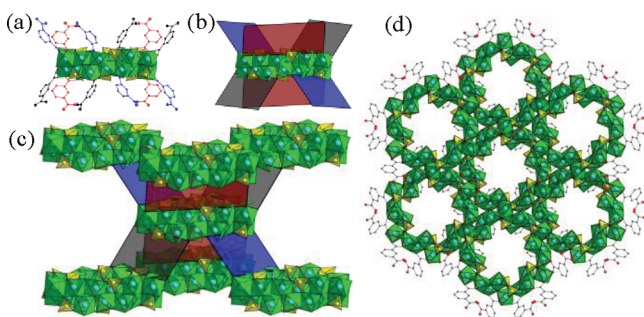


Figure 2. View of the wheel unit above and below which there are six pairs of ip ligands (a). Each pair of ip ligands simplified as a colored rectangle (b). Each wheel linking six neighbors (c). 3D structures of **1** and **2** along the c axis (d).

ligands. Six pairs of ip ligands connect six M^{II}_{24} wheels (each pair of ip ligands is represented by a colored rectangle; Figure 2b,c), with each ip ligand bound to four M^{II} ions, resulting in 3D M^{II}_{24} -wheel-based coordination polymers (Figures 2d and S1 in the Supporting Information), with void spaces being occupied by lattice DMSO, EtOH, and water molecules. From a topological point of view, the M^{II}_{24} wheel is a structural node and each pair of ip ligands is a linker; the frameworks of the two 3D coordination polymers can then be simplified to a 3D α -polonium-type structure of $4^{12}6^3$ topology (Figure S2 in the Supporting Information).

The molar direct-current (dc) magnetic susceptibilities (per M^{II}_{24} unit) of microcrystalline samples of **1**-guests and **2**-guests measured in the temperature range 2–300 K under 0.1 T external field are shown in Figure 3a. The $\chi_M T$ value for **1**-guests at 300 K are $68.26 \text{ cm}^3 \text{ K mol}^{-1}$, significantly higher than the spin-only value expected for 24 isolated Co^{II} ions with $S = 3/2$ ($45.00 \text{ cm}^3 \text{ K mol}^{-1}$; $g = 2.0$). It gives a realistic g_{Co} value of 2.46 if we assume that the ions are uncoupled; this

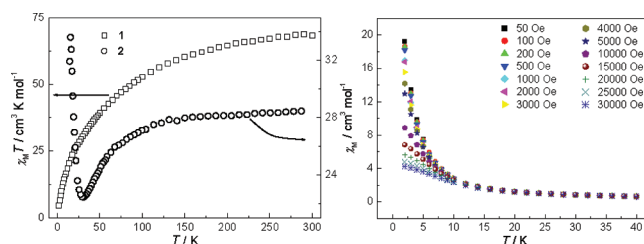


Figure 3. $\chi_M T$ versus T plots of **1**-guests and **2**-guests measured at 1 kOe external field (a) and field-dependent magnetic susceptibilities of **2**-guests in the 2–40 K temperature range (b).

result is attributed to the unquenched orbital contributions of Co^{II} ions in an octahedral field. Upon temperature cooling, the $\chi_M T$ value monotonously decreases to attain a value of $4.51 \text{ cm}^3 \text{ K mol}^{-1}$ at 2 K, which indicates dominant antiferromagnetic interactions within and between the Co_{24} wheels; meanwhile, spin–orbital coupling effects may also influence the overall profile. A low-temperature M versus H plot (Figure S5 in the Supporting Information) further confirms the overall antiferromagnetic interactions. The $\chi_M T$ value for **2**-guests at 300 K is $28.43 \text{ cm}^3 \text{ K mol}^{-1}$, slightly higher than the spin-only value expected for 24 isolated Ni^{II} ions with $S = 1$ ($24.00 \text{ cm}^3 \text{ K mol}^{-1}$; $g = 2.0$) and giving a realistic g_{Ni} value of 2.18. The $\chi_M T$ value generally decreases to $22.45 \text{ cm}^3 \text{ K mol}^{-1}$ at 20 K and then rises sharply to reach a value of $33.62 \text{ cm}^3 \text{ K mol}^{-1}$ at 3 K, followed by a sudden drop to $31.93 \text{ cm}^3 \text{ K mol}^{-1}$ at 2 K. This profile and the θ value (-6.6 K ; Figure S4 in the Supporting Information) indicate dominant antiferromagnetic interactions within the Ni_{24} wheel; the rise of the $\chi_M T$ value at low temperature implies that extrinsic intrawheel antiferromagnetic interactions may be the result of competitive ferro- and antiferromagnetic interactions between Ni^{II} ions that lead to a ground-state spin ($S_T \sim 6$ corresponding to the $\chi_M T$ value at a minimum) and adjacent wheels ferromagnetically coupled or antiferromagnetically coupled with spin canting. The significant magnetic ground state is further supported by the low-temperature M versus H plot (Figure S6 in the Supporting Information), which shows a quick increase (compared with **1**-guests) at relatively low external fields. The value of the magnetization ($12\text{--}14 \mu_B$ per Ni^{II}_{24} unit) after this quick increase confirms the presence of dominant antiferromagnetic interactions that are uncompensated for by ferro- and antiferromagnetic interactions within the **2** wheel.

In order to elucidate the low-temperature magnetic behavior, field-dependent magnetic susceptibilities of **1**-guests and **2**-guests at temperature range of 2–40 K have been measured. Interestingly, only **2**-guests undergoes field-dependent behavior

(Figure 3b), whose magnetic susceptibilities increase with decreasing external fields, which further confirms the ground state of 2-guests and canted interwheel antiferromagnetic interactions. Because of the nonsignificant anisotropy of Ni^{II} ions, the presence of spin canting is probably due to the noncollinear interwheel spin structure or Dzyaloshinskii–Moriya interactions.¹¹ It should be mentioned that the field-dependent behavior of 2-guests may also be a consequence of the zero-field-splitting effect associated with Ni^{II} ions. On the other hand, the monotonous increases in χ_M upon cooling for 1-guests and 2-guests indicate that they are not antiferromagnetically ordered above 2 K (Figure S7 in the Supporting Information). Meanwhile, the nonzero values at 2 K and the monotonous increases in χ_M imply that the ground state of 2-guests is significantly larger than that of 1-guests. To clarify this situation, alternating-current (ac) susceptibility measurements were performed in zero applied dc field and 3 Oe ac field oscillating at 1 and 99.9 Hz, respectively (Figures S8 and S10 in the Supporting Information). Extrapolations of the $\chi_M''T$ versus T plots to 0 K give values of 4.61 and 39.84 cm³ K mol⁻¹ for 1-guests and 2-guests (Figures S9 and S11 in the Supporting Information), respectively, which agree well with the observed ones for $\chi_M T$ at 2 K, indicating magnetic $S = 1$ and 7–8 ground states for 1-guests and 2-guests, respectively. The in-phase signals are frequency-independent (and without peaks), and no out-of-phase signals are observed down to 2 K; thus, above this temperature, there is no magnetization relaxation.

Because of the anisotropic nature of the Co^{II} ion, it is hard to figure out the spin topology of 1-guests and which type of exchange pathways should dominate, but for 2-guests, the correlation of the observed magnetic properties with the structure can be rationally realized. For octahedral nickel(II) complexes, $d_{x^2-y^2}$ and d_{z^2} are the two magnetic orbitals. The dominant superexchange pathway between two Ni^{II} centers (in the Ni–O–Ni species) involves $d_{x^2-y^2}$ orbitals of Ni^{II} ions and p orbitals of the bridging O atom, which results in antiferromagnetic exchange, whose coupling integral ($-J$) increases as the Ni–O–Ni bridge angle and hence the Ni \cdots Ni distance increases, while d_{z^2} orbitals interact ferromagnetically through space and the magnitude of exchange depends on the distance between the Ni^{II} centers. Thus, increases of the Ni–O–Ni bridge angle and hence the Ni \cdots Ni distance simultaneously strengthen antiferromagnetic coupling and weaken ferromagnetic coupling. The ferromagnetic crossover point for a Ni–O–Ni bridge angle is 96°; however, the real Ni–O–Ni bridge angle leading to dominant antiferromagnetic interactions usually exceeds 99°. As shown in Figure S12 and Table S2 in the Supporting Information, the bond angles of Ni1–O–Ni4 and Ni2–O–Ni3 are less than 98°, while those of Ni1–O–Ni3, Ni2–O–Ni4, and Ni3–O–Ni4 are larger than 100°. Thus, we can simply assign the exchanges between Ni1 and Ni4 and between Ni2 and Ni3 to be ferromagnetic and those between Ni1 and Ni2/Ni3 and between Ni4 and Ni2/Ni3 to be antiferromagnetic. The significant ground-state spin determined by both dc and ac magnetic susceptibility data indicates that antiferromagnetic interactions may be noncollinear.

In summary, we have synthesized and characterized two 3D coordination polymers based on by far the largest Co^{II}₂₄ and Ni^{II}₂₄ wheel-like building units. The wheels have aesthetically pleasing structure and Ni^{II}₂₄ has a ground-state spin $S \sim 6$ due to both ferro- and antiferromagnetic interactions within the Ni^{II}₂₄ wheel. Further evidence shows that interwheel interactions in the two complex frameworks are antiferromagnetic,

but in 2-guests they are canted and therefore show weak ferromagnetism. The two compounds show tremendous changes in bulky magnetic properties and magnetic ground states, implying the possibility of tuning magnetic properties by slight structure changes.

■ ASSOCIATED CONTENT

● Supporting Information

Experimental details, figures, crystal data in CIF format. This material is available free of charge via the Internet at <http://pubs.acs.org>.

■ AUTHOR INFORMATION

Corresponding Author

*E-mail: taojun@xmu.edu.cn.

Notes

The authors declare no competing financial interest.

■ ACKNOWLEDGMENTS

We are thankful for financial support from the NNSF of China (Grants 90922012, 20971106, and 21021061) and the Specialized Research Fund for the Doctoral Program of Higher Education (Grant 20110121110012).

■ REFERENCES

- (1) (a) Gatteschi, D.; Sessoli, R.; Villian, J. *Molecular Nanomagnets*; Oxford University Press: Oxford, U.K., 2006. (b) Murrie, M. *Chem. Soc. Rev.* **2010**, *39*, 1986.
- (2) (a) Murugesu, M.; Habrych, M.; Wernsdorfer, W.; Abboud, K. A.; Christou, G. *J. Am. Chem. Soc.* **2004**, *126*, 4766. (b) Bai, Y.-L.; Tao, J.; Wernsdorfer, W.; Sato, O.; Huang, R.-B.; Zheng, L.-S. *J. Am. Chem. Soc.* **2006**, *128*, 16428. (c) Bai, Y.-L.; Tao, J.; Huang, R.-B.; Zheng, L.-S. *Angew. Chem., Int. Ed.* **2008**, *47*, 5344. (d) Mohamedally, K. *Chem. Soc. Rev.* **2009**, *38*, 1353.
- (3) (a) Chiolerio, A.; Loss, D. *Phys. Rev. Lett.* **1998**, *80*, 169. (b) Cornia, A.; Jansen, A. G. M.; Affronte, M. *Phys. Rev.* **1999**, *B60*, 12177. (c) Ramsey, C. M.; Del Barco, E.; Hill, S.; Shah, S. J.; Beedle, C. C.; Hendrickson, D. N. *Nat. Phys.* **2008**, *4*, 277.
- (4) (a) Dearden, A. L.; Parsons, S.; Winpenny, R. E. P. *Angew. Chem., Int. Ed.* **2001**, *40*, 151. (b) Foguet-Albiol, D.; Abboud, K. A.; Christou, G. *Chem. Commun.* **2005**, 4282.
- (5) King, P.; Stamatatos, T. C.; Abboud, K. A.; Christou, G. *Angew. Chem., Int. Ed.* **2006**, *45*, 7379.
- (6) Liu, C.-M.; Zhang, D.-Q.; Hao, X.; Zhu, D.-B. *Chem.—Eur. J.* **2011**, *17*, 12285.
- (7) Bai, Y.-L.; Tangoulis, V.; Huang, R.-B.; Zheng, L.-S.; Tao, J. *Chem.—Eur. J.* **2009**, *15*, 2377.
- (8) Tasiopoulos, A. J.; Vinslava, A.; Wernsdorfer, W.; Abboud, K. A.; Christou, G. *Angew. Chem., Int. Ed.* **2004**, *43*, 2117.
- (9) (a) Müller, A.; Koop, M.; Bögge, H.; Schmidtman, M.; Beugholt, C. *Chem. Commun.* **1998**, 1501. (b) Tsuda, A.; Hirahara, E.; Kim, Y.-S.; Tanada, H.; Kawai, T.; Aida, T. *Angew. Chem., Int. Ed.* **2004**, *43*, 6327.
- (10) (a) Dan-Hardi, M.; Serre, C.; Fort, T.; Rozes, L.; Maurin, G.; Sanchez, C.; Férey, G. *J. Am. Chem. Soc.* **2009**, *131*, 10857. (b) Sumida, K.; Hill, M. R.; Horike, S.; Dailly, A.; Long, J. R. *J. Am. Chem. Soc.* **2009**, *131*, 15120.
- (11) (a) Li, Z.-X.; Zhao, J.-P.; Sanudo, E. C.; Ma, H.; Pan, Z.-D.; Zeng, Y.-F.; Bu, X.-H. *Inorg. Chem.* **2009**, *48*, 11601. (b) Li, J.-R.; Yu, Q.; Tao, Y.; Bu, X.-H.; Ribas, J.; Batten, S. R. *Chem. Commun.* **2007**, 2290.
- (12) (a) Nanda, K. K.; Das, R.; Venkatsubramanian, K.; Nag, K. *Proc. Indian Acad. Sci. (Chem. Sci.)* **1994**, *106*, 673. (b) Boyd, P. D. W.; Martin, R. L.; Schwarzenbach, G. *Aust. J. Chem.* **1988**, *41*, 1449 and references cited therein.